Optimal Design of eVTOLs for Urban Mobility using Analytical Target Cascading (ATC)

Prajwal K. Chinthoju*
University of Illinois at Urbana Champaign, Urbana, IL 61801, USA

Yong Hoon Lee†
The University of Memphis, Memphis, TN 38152, USA

Ghanendra K. Das‡ and Kai A. James§
Georgia Institute of Technology, Atlanta, GA 30332, USA

James T. Allison¶
University of Illinois at Urbana Champaign, Urbana, IL 61801, USA

Over the past few decades, multidisciplinary design optimization (MDO) techniques have shown great potential in generating optimal designs for complex system of systems. Monolithic MDO methods that formulate the design problem as a single optimization problem are effective, but present challenges in coordination. On the other hand, distributed MDO methods decompose the design problem into different optimization problems and hence offer more modularity and flexibility, especially when implemented by teams of optimization specialists. In this article, one such distributed MDO method, Analytical Target Cascading (ATC), is investigated as a candidate for the design of electric Vertical Take Off and Landing aircraft (eVTOL). Design of eVTOLs for urban mobility has been a subject of immense interest over the past decade. eVTOLs offer many advantages over conventional modes of urban transport such as reduced environmental impact, utilization of vertical space for transportation, and competitive cost of transportation. Most current efforts for eVTOL design are in relatively early stages. Hence, distributed MDO methods that can effectively consider complex interactions between different subsystems and disciplines can help support eVTOL design efforts. In this study, ATC is implemented to optimize the total cost per flight for a simple mission, involving take-off to a set altitude, cruising at constant velocity for a range of 50-150 km, and landing, all while carrying a given payload. The key design parameters that are optimized as a part of this study are the mass of aircraft and individual subsystems, cruise velocity, wingspan, and radius of the propeller. Furthermore, a comparison of the resulting optimal solutions using ATC and monolithic MDO methods is presented. General observations are also articulated regarding potential computational advantages, such as parallelism and tailored solution algorithms, as well as organizational considerations, such as distributed iterative subproblem formulation refinement conducted by human subject matter experts and team coordination.

I. Nomenclature

m_x	=	mass of component x
r_{prop}	=	radius of propeller
c_{prop}	=	chord length of propeller
b_{span}	=	wingspan
V	=	cruise velocity

*Graduate Researcher, Industrial & Enterprise Systems Engineering, 104 S Mathews Ave, 406 TB, Urbana, IL 61801, AIAA Student Member
†Assistant Professor, Department of Mechanical Engineering, 3815 Central Ave, 322D ES, Memphis, TN 38152, AIAA Member.
‡Graduate Researcher, School of Aerospace Engineering, 275 Ferst Dr NW, 212 Weber, Atlanta, GA 30313, AIAA Student Member
§Associate Professor, School of Aerospace Engineering, 275 Ferst Dr NW, 212 Weber, Atlanta, GA 30313, AIAA Member
¶Associate Professor, Industrial & Enterprise Systems Engineering, 104 S Mathews Ave, 313 TB, Urbana, IL 61801, AIAA Senior Member

AR	=	wing aspect ratio
root_{AoA}	=	angle of attack at root of the wing
P_{hover}	=	power required to be generated by each motor during the hover phase
η_{motor}	=	efficiency of motor

II. Introduction

Multidisciplinary design optimization (MDO) has gained significant attention for system design applications over the past few decades. Early MDO methods primarily focused on incorporating additional disciplines into structural optimization problems [1], later expanding to engineering-scale applications such as aircraft wing design [2], spacecraft [3], and complete business jets [4]. A comprehensive introduction to MDO methods is available in Martins and Lambe [5]. eVTOL design can be modeled as an engineering system design optimization problem, requiring the coordination of various subsystems such as propulsion, wings, motors, and batteries while simultaneously optimizing for system-level objectives, such as cost per flight or total aircraft mass. Although numerous MDO methods can help address complex optimization problem of designing an eVTOL, it is crucial to select a technique that considers the physical and design decision interactions between different subsystems in the context of overall system utility.

MDO methods can be categorized into two main types, monolithic and distributed, depending upon the number of optimization problems in the overall problem formulation [5, 6]. Monolithic methods solve a single optimization problem, while distributed methods divide it into multiple formulations according to a partitioning criterion, such as physics discipline or physical subsystems. One early motivation for developing distributed MDO methods was to mirror engineering design organizations, wherein various teams work on distinct subsystems or disciplines while maintaining strong communication channels across teams [1]. Isolation of different disciplines/subsystems in distributed MDO methods allows engineering teams to work independently (on optimization subproblems) yet synergistically (informed by system optimization results) to support engineers in making design decisions that align with improving overall system value.

Engineering design optimization studies involve more than numerical solution. One model for describing the usually iterative process is termed the Engineering Design Optimization (EDO) Problem Formulation Cycle (PFC) that involve the following phases: (1) problem formulation construction, (2) problem formulation analysis, (3) problem solution, and (4) solution analysis. The EDO PFC was first introduced in an undergraduate EDO course [7] as a strategy to accelerate the process of learning practical skill in performing EDO studies of value to engineering organizations, and has been used to inform studies of EDO methods [8]. While computational optimization methods automate the solution procedure in Step (3), the other steps (1, 2, and 4) require significant human effort, especially when multiple interdisciplinary teams are involved in collaborative design practices.

While distributed MDO approaches can be more computationally expensive than monolithic solution strategies (EDO PFC Step (3)), distributed methods have other potential advantages that could reduce the overall time and effort required to conduct system design optimization studies. Specifically, distributed MDO methods partition the system optimization problem into multiple separate disciplinary domain or subsystem optimization subproblems. This frees individual engineers or specialist groups to focus on constructing, solving, and refining optimizing subproblem formulations. In contrast, monolithic optimization approaches require that the larger system design team negotiates and agrees upon a single system-wide problem formulation. Distributed MDO methods can help to reduce the complexity of the human-centered EDO PFC tasks, including agreeing on a formulation and iteratively refining the solution implementation and the formulation. In other words, distributed MDO can be advantageous in the context of a team design environment, due to their independent, modular, and parallel nature. In addition to supporting parallel computing, distributed MDO supports parallel execution of significant human expert tasks. This article introduces the concept that distributed MDO may have broader value in an organizational context due to support of parallel human tasks, but rigorous studies of a range of organizational types, system design projects, and MDO strategies are needed to confirm this potential benefit of MDO.

Analytical Target Cascading (ATC) is a distributed MDO method that emulates the hierarchical structure of some engineering organizations, or hierarchical relationships between subsystems and components within a larger system [9–11], (organizational structure sometimes, but not always, aligns with system structure [12]). ATC is a multi-level MDO formulation that involves propagating targets and responses through the hierarchical structure until a consistent solution is achieved. The targets and responses at each iteration are the result of the system and the individual optimization problems, respectively, which in turn ensures that the value of the overall objective function is minimized. Several different versions of ATC formulations exist in the literature; the formulation used here is based on the version

introduced by Tosserams et al. [13].

The specific problem of eVTOL vehicle design was chosen for this study owing to the rich interactions between its different subsystems. The concept of an eVTOL vehicle originated with the need to develop an urban transport aircraft that functions well in both lift and cruise phases of flight while being powered by a battery. Although helicopters can take off and land vertically, the performance of helicopters during the cruise phase is lower than other aircraft [14]. eVTOL vehicles combine the vertical take-off and landing functionality of helicopters with the cruise phase efficiency of conventional aircraft. There are many proposed configurations of eVTOLs, including the tilt wing, tilt-rotor, and multi-rotor designs. This study focuses on the design of a tilt-wing eVTOL aircraft. There are several crucial subsystems within an eVTOL that are inherently coupled with each other. For example, the thrust that is needed during the hover phase of the mission depends on the motor design as well as the propeller design. Hence, it is essential that the motor and the propeller are designed considering all of the interactions between these subsystems. These interactions add to the complexity of engineering design problems and, therefore, eVTOL design optimization efforts.

The focus of this study is to assess the feasibility of using ATC for the complex engineering-level problem of eVTOL design optimization and to compare the results of ATC with optimal solutions generated from monolithic MDO formulation. The potential value of distributed MDO methods is then articulated with this comparison, both in the context of computational performance and broader use within human design organizations.

III. Methodology

A. Analytical target Cascading

ATC was originally developed not as an MDO method but as an effective approach to cascade targets through a hierarchical structure to support concurrent subsystem development activities while still guiding the process toward system optimality [11]. Target cascading strategies have been used in industry systems engineering efforts, and ATC was inspired by these existing strategies. It provides a formal way to iteratively refine design targets that accounts for system interactions. The initial formulations for ATC included propagating system-level targets to the subsystems. If a target for a subsystem cannot be achieved, the subsystem returns a response to that target that aims to minimize its deviation from the response. This information can then be used by parent subproblems to adjust the target, balancing subsystem capabilities and overall system design considerations.

With the advent of important advancements to ATC theory and methods (e.g., [13, 15]), as well as comparative analyses of ATC and established MDO methods (e.g., [16, 17]), ATC can now be understood as a subclass of MDO formulations. Specifically, ATC is an MDO formulation that includes a consistently-applied system-level objective function, hierarchically distributed optimization subproblems, and an appropriate coordination algorithm for guiding subproblem solutions toward convergence, resulting in a system-optimal solution that satisfies consistency requirements across subproblems. Before we formulate the optimization problem, we need to identify the design variables and split them into shared design variables and coupling variables. Additionally, each discipline can also have state variables that are local to that specific discipline or component and are not interfaced with other subsystems. The general ATC formulation in Eq. (1), based on the formulation introduced in Ref. [13], lays out the objective function and constraints for each subproblem of a typical ATC formulation:

$$
\begin{aligned}
\underset{\bar{\mathbf{x}}_{ij}}{\text{minimize:}} \quad & f_{ij}\left(\bar{\mathbf{x}}_{ij}\right) + \phi\left(\mathbf{t}_{ij} - \mathbf{r}_{ij}\right) + \sum_{k \in C_{ij}} \phi\left(\mathbf{t}_{(i+1)k} - \mathbf{r}_{(i+1)k}\right) \\
\text{subject to:} \quad & \mathbf{g}_{ij}\left(\bar{\mathbf{x}}_{ij}\right) \leq \mathbf{0} \\
& \mathbf{h}_{ij}\left(\bar{\mathbf{x}}_{ij}\right) = \mathbf{0} \\
\text{with respect to:} \quad & \mathbf{r}_{ij} = \mathbf{a}_{ij}\left(\mathbf{x}_{ij}, \mathbf{t}_{(i+1)k_1}, \cdots, \mathbf{t}_{(i+1)k_{C_{ij}}}\right) \\
& \bar{\mathbf{x}}_{ij} = \left[\mathbf{x}_{ij}, \mathbf{r}_{ij}, \mathbf{t}_{(i+1)k_1}, \cdots, \mathbf{t}_{(i+1)k_{C_{ij}}}\right],
\end{aligned}
\tag{1}
$$

where $\bar{\mathbf{x}}_{ij}$ is the vector of the design variables for subsystem j, at level i, f_{ij} is the local objective function at that subsystem, $\mathbf{t}_{ij}$, $\mathbf{r}_{ij}$ are the targets and responses of subsystem j with its parent, respectively, $\mathbf{t}_{(i+1)k}$, $\mathbf{r}_{(i+1)k}$ are the targets and responses of subsystem k in level $i+1$ with its parents (in level i), and $\mathbf{g}_{ij}$ and $\mathbf{h}_{ij}$ are the local constraints of the subsystem j at level i. $t_{(i+1)k_l}$ where $l = [1, 2, 3 \ldots C_{ij}]$ represent the targets that are passed from level i to subsystem l in level $(i+1)$

The coordination algorithm used in this study is the same as the one presented in Ref. [15], which introduces Augmented Lagrangian Coordination (ALC), a generalization of ATC. This coordination method uses a penalty function

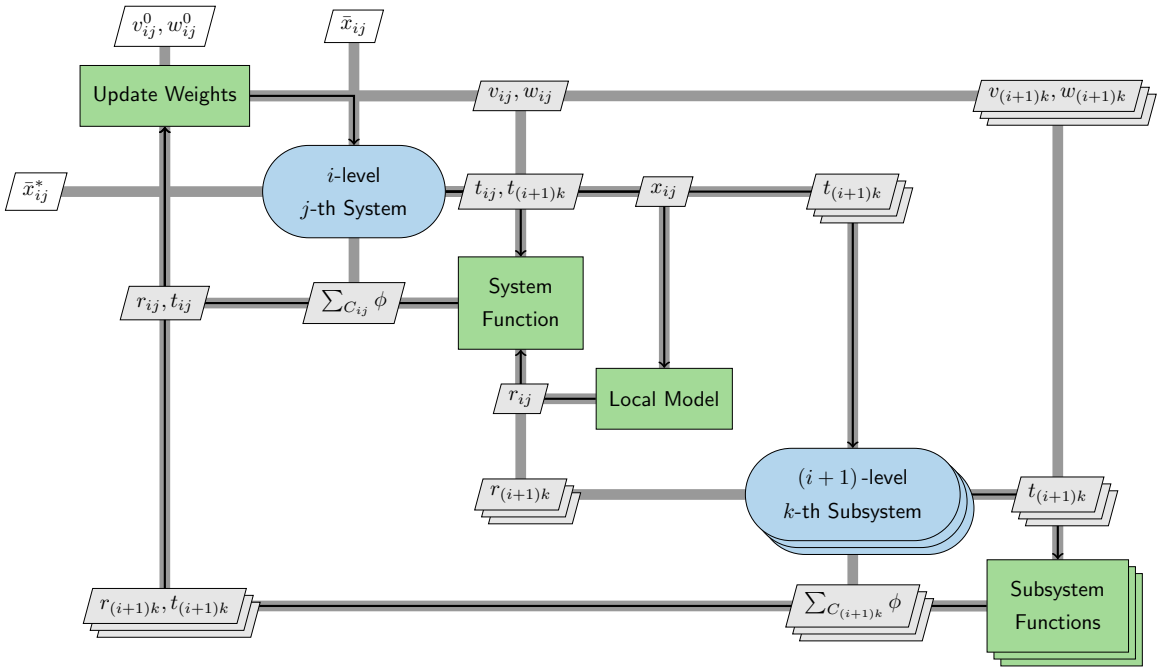

Fig. 1 ATC formulation recursively represented in extended design structure matrix (XDSM) [18]

with linear and quadratic terms to minimize error between targets and responses. The weights $\mathbf{v}$ and $\mathbf{w}$ govern the behavior of the linear and quadratic penalty terms, respectively. This penalty function is defined in Eq. (2):

$$\phi\left(\mathbf{t}_{ij} - \mathbf{r}_{ij}\right) = \mathbf{v}_{ij}^{\mathsf{T}}\left(\mathbf{t}_{ij} - \mathbf{r}_{ij}\right) + \left\|\mathbf{w}_{ij} \otimes \left(\mathbf{t}_{ij} - \mathbf{r}_{ij}\right)\right\|_2^2. \tag{2}$$

Here, the $\otimes$ operator refers to the Hadamard product (element-wise product of two equal-dimension matrices that produces another matrix of same dimension). For a given set of weights, all subproblems are solved in a coordinated way with the goal of finding a consistent and system-optimal solution. After completion of iterative subproblem solutions, the weights $\mathbf{v}$ and $\mathbf{w}$ are updated to help reduce error between targets and responses. The update formulas used here are:

$$\begin{aligned} \mathbf{v}^{k+1} &= \mathbf{v}^k + 2\mathbf{w}^k \otimes \mathbf{w}^k \otimes \mathbf{q}^k \\ w_i^{k+1} &= \begin{cases} w_i^k & \text{if } \left|q_i^k\right| \le \gamma \left|q_i^{k-1}\right| \\ \beta w_i^k & \text{if } \left|q_i^k\right| > \gamma \left|q_i^{k-1}\right|, \end{cases} \end{aligned} \tag{3}$$

where q_{ij}^k is $\left(\mathbf{t}_{ij} - \mathbf{r}_{ij}\right)$ at the k-th iteration. In Eq. (3), the ALC coordination method increases the penalty weights only if the residual of the constraint has not converged by a ratio of γ (i.e., weights are updated only when necessary). This helps to prevent the weights from growing to values large enough to cause problem ill conditioning. Along with γ, β is another hyper parameter that can be tuned in ATC and ALC implementations. β controls the rate at which the quadratic weights grow over the sequence of optimization solutions.

The flowchart of a hierarchical ATC implementation is illustrated in Fig. 1. The ATC coordination algorithm first begins by solving the system level optimization problem, iterates through all the subproblems and solves the respective individual optimization problems based on the targets set by the system level problem. After each one of these cycles, the residuals for both the consistency and disciplinary constraints are computed and the weights are updated accordingly. This cycle is repeated until all the consistency constraint tolerances are met. Please note that other subproblem solution patterns, such as solving all subproblems in parallel regardless of level, have been investigated.

B. eVTOL Problem Formulation

The primary requirement for the vehicle in this study is to perform the simple mission shown in Fig. 2. The mission starts with a 90 second ascent phase, followed by a cruise phase at a constant velocity for a range between 50-150 km,

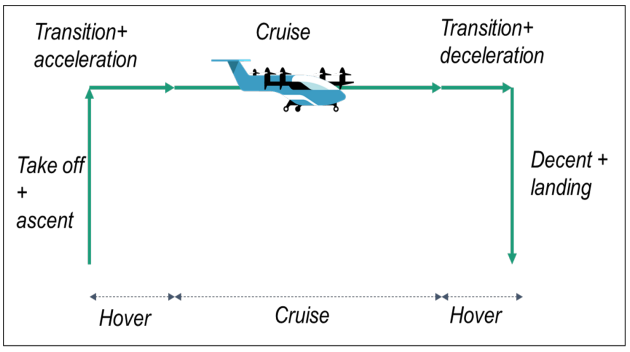

Fig. 2 Simple mission formulation

Table 1 System level design variables

$x_\#$	Symbol	Design variable	Units	$x_\#$	Symbol	Design variable	Units
1	r_{prop}	Radius of propeller	m	6	E_{reserve}	Energy required for reserve mission	J
2	V	Cruise velocity	m/s	7	b_{span}	Wingspan	m
3	m_{batt}	Mass of battery	kg	8	ω_{hover}	Hover rpm	rpm
4	m_{motor}	Mass of motors	kg	9	η_{motor}	Efficiency of motor	-
5	MTOW	Maximum takeoff weight	N	10	m_{gb}	Mass of gearbox	kg

and then ends with a 90 second descent phase. For simplicity of the problem formulation, acceleration and deceleration phases are not modeled and ascent and descent phases are modeled as hover.

A reserve mission is also modeled to include additional safety in aircraft operation. The reserve mission involves an additional 20 min loiter at cruise velocity. This mission constraints the minimum battery capacity of the included battery in the aircraft. The motor sizing is constrained by the maximum power required during the mission (which corresponds to the hover power). Other system level constraints included in this problem are given in the following section.

C. System-level Modeling

There are two system level objective functions that are considered here for eVTOL design. One is the mass of the aircraft (excluding payload) and the other one is the cost per flight. These objective functions are computed using the Vahana eVTOL model developed by the Airbus A3 program [19]. While the cost per flight strongly correlates with the mass of the aircraft, it is not strictly linear. In all the results analyzed in this study we use the cost of aircraft as the objective function. The cost per flight modeling encompasses different cost components such as tooling cost, material cost, battery cost, motor cost, servo cost, avionics cost, operational cost, electricity cost, and other factors. Costs which span the life cycle of the aircraft are amortized assuming 10 years of operational life and 600 hrs operation per year.

The purpose of the ATC system level formulation is to optimize the system-level objective function while simultaneously determining appropriate targets for child subsystems. The system level subproblem also includes any constraints on design variables that are not included in subsystem level formulations. The system-level design variables are articulated in Table 1, and the system-level subproblem formulation is:

$$
\begin{aligned}
\underset{x}{\text{minimize:}} \quad & \text{Cost per flight} + \sum_{k\in[2,3,4]} \phi\left(\mathbf{t}_{2k} - \mathbf{r}_{2k}\right) \\
\text{subject to:} \quad & m_{\text{total}} \leq \text{MTOW} \\
& E_{\text{reserve}} \leq 0.95 E_{\text{batt,cap}} \\
& T \leq T_{\text{max}} \\
\text{with respect to:} \quad & x = \left[r_{\text{prop}}, V, m_{\text{batt}}, m_{\text{motor}}, \text{MTOW}, E_{\text{reserve}}, S_{\text{wing}}, \text{RPM}_{\text{motor}}, \eta_{\text{motor}}, m_{\text{gb}}\right],
\end{aligned}
\tag{4}
$$

where m_{total} is the overall mass of the eVTOL vehicle, MTOW is the maximum take off weight, E_{reserve} is the energy required in reserve mission, $E_{\text{batt,cap}}$ is the maximum battery capacity, T is the motor torque, and T_{max} is the maximum motor torque. The subscripts in the above formulation follows the convention presented in Eq. (1), and will be used consistently ($k \in [2, 3, 4]$) throughout this study.

D. Component Modeling

Vehicle components (or subsystems) are the basis for the remaining ATC subproblems. This ATC formulation is limited to two levels, so all remaining subproblems are at level 2. Other partitionings are possible, including further decomposition into disciplinary subproblems.

Design of an eVTOL involves several complex subsystems, but here we restrict ourselves to modeling a few key components, namely: motor, gearbox, wing, and propeller. Other components such as battery and fuselage are modeled directly in the system level objective function using simple analytical models. The models chosen here are relatively low fidelity; an example of a higher-fidelity eVTOL MDO study is presented in Sarojini et al. [20]. The models used here provide enough richness to capture important trends in the system design problem, but are computationally inexpensive. For optimization studies with the goal of producing numerical results that could inform design decisions directly, higher fidelity models should be used.

1. Motor

All eight electric motors used in this eVTOL vehicle are identical and are modeled using an rpm-torque-efficiency map. The sizing of the motor is determined by the maximum torque that the motor can produce [21]. The motor mass is sized using the analytical relation given by Eq. (5):

$$m_{\text{motor}} = 0.03928 T_{\text{max}}^{0.8587}, \tag{5}$$

where m_{motor} is the mass of the motor (in pound-mass) and the maximum torque T_{max} is expressed in lb-ft.

The system-level subproblem constrains motor sizing via a torque constraint, as shown in Eq. (4). This is implicitly enforced in the subproblems through ATC coordination. The torque constraint was placed in the system-level subproblem instead of the motor subproblem to eliminate the need to compute hover power (needed to determine the maximum torque) in the motor subproblem. The purpose of the motor subproblem is to output an efficiency for a given rpm and torque. Each tilt-wing of the aircraft has four propellers, resulting in eight total required motors. The motor model queries the rpm-torque-efficiency map and provides estimates for efficiency given a torque and speed operating point. The optimization formulation for this subsystem is as follows:

$$\begin{aligned} \underset{\mathbf{x}}{\text{minimize:}} \quad & \phi\left(\mathbf{t}_{12} - \mathbf{r}_{12}\right) \\ \text{subject to:} \quad & \texttt{efficiency-map}\left(\text{RPM}_{\text{motor}}, T\right) - \eta_{\text{motor}} = 0 \\ \text{with respect to:} \quad & \mathbf{x} = \left[\text{RPM}_{\text{motor}}, \eta_{\text{motor}}\right], \end{aligned} \tag{6}$$

where `efficiency-map` represents a look-up table.

2. Gearbox

The gearbox model uses an analytical sizing model given the power transmitted, motor rpm, and propeller rpm [22]. The Vahana model, from which much of the formulation used in this study is inherited, does not use a gearbox as it adds additional weight. However, the addition of gearboxes can also increase the overall efficiency of the aircraft by allowing operation of the electric motor at a higher efficiency point. This can in turn reduce the battery weight, thereby reducing the mass of the system leading to a more optimal solution. This trade-off is observed in the optimal solutions and including a gearbox indeed results in a system with lower mass than the case where the electric motor is directly coupled to the propeller. The analytical model for the gearbox sizing is given in Eq. (7):

$$m_{\text{gb}} = 0.453592 \kappa \left(\text{hp}^{0.76}\right) \frac{\omega_{\text{motor}}^{0.13}}{\omega_{\text{prop}}^{0.89}}, \tag{7}$$

where κ is an index given by the current development progress as 94 and hp is the power transmitted in HP.

The optimization formulation for this subsystem is as follows:

$$\begin{aligned} \underset{\mathbf{x}}{\text{minimize:}} \quad & \phi\left(\mathbf{t}_{13} - \mathbf{r}_{13}\right) \\ \text{subject to:} \quad & m_{\text{gb}} = \texttt{gearbox-sizing}\left(r_{\text{prop}}, V, \text{MTOW}, S_{\text{wing}}, \text{RPM}_{\text{motor}}, \eta_{\text{motor}}, m_{\text{gb}}\right) \\ \text{with respect to:} \quad & \mathbf{x} = \left[r_{\text{prop}}, V, \text{MTOW}, S_{\text{wing}}, \text{RPM}_{\text{motor}}, \eta_{\text{motor}}, m_{\text{gb}}\right], \end{aligned} \tag{8}$$

3. Wing

The wing of the aircraft is modeled using a constant lift coefficient. Using the lift coefficient and the wing surface area, the lift generated at stall can be computed. For a given value of stall velocity (assumed to be 35 m/s), the minimum area of the wing that can support the weight of the aircraft can be computed. The formulation for this subsystem is as follows:

$$\begin{aligned} \underset{x}{\text{minimize:}} \quad & \phi\left(\mathbf{t}_{14} - \mathbf{r}_{14}\right) \\ \text{subject to:} \quad & \mathrm{S_{wing}} \leq \frac{\mathrm{MTOW} \times \mathrm{g}}{\frac{1}{2}\rho\, \mathrm{V_{stall}^2\, C_L}} \\ \text{with respect to:} \quad & \mathbf{x} = \left[\mathrm{MTOW}, \mathrm{S_{wing}}\right], \end{aligned} \tag{9}$$

where g is the acceleration due to gravity, ρ is the air density, and C_L is the aircraft lift coefficient.

E. Propeller modeling and power calculation

To simplify the complexity of the ATC formulation, the propeller is modeled within the system level subproblem and not as a separate subsystem. The propulsion system includes eight propellers with four blades each. For determining the thrust generated by each propeller, actuator disk (AD) theory is used. The time allotted for the hover phase of the mission is 3 minutes in which the aircraft needs to takeoff vertically and reach the cruise velocity. The thrust required during hover phase is essentially the sum of weight of the aircraft and mass times the horizontal acceleration required for achieving cruise velocity. Once the thrust required is known, the model uses the solidity of the propeller and other parameters such as radius, hover rpm, and chord length, and computes the power and torque generated using Eq. (10):

$$P_{\text{hover,max}} = n_{\text{prop}} T_{\text{prop}} \left(k \sqrt{\frac{T_{\text{prop}}}{2\pi\rho_\infty r_{\text{prop}}^2}} + \sigma \frac{C_{\text{d0}}}{8} \frac{{v_{\text{tip}}}^2}{\frac{T_{\text{prop}}}{\pi\rho_\infty r_{\text{prop}}^2}} \right), \tag{10}$$

where C_{d0} and P_∞ are the sectional drag coefficient and free stream air density respectively. A sectional drag coefficient of 0.012 is used based on a NACA0012 airfoil blade profile. v_{tip} is the tip speed of the propeller which is constrained to Mach 0.6. k is an empirical correction factor included to correlate the power computed from AD theory with experimental findings [23]. The torque required can be computed as the ratio of power consumed to angular speed of the propeller Eq. (11):

$$Q_{\text{hover, max}} = \frac{P_{\text{hover,max}}}{\omega}. \tag{11}$$

As an alternative, blade element momentum (BEM) theory could also be used to compute the power consumed by the propeller. In this method, the propeller blade is divided into a discrete number of subsections. The elemental thrust generated by each discrete blade element can be computed in terms of the angle of attack, lift and drag forces. This, combined with the axial and angular conservation of momentum from the actuator disk theory, can be used to compute the axial flow factors iteratively [24].

Blade element momentum theory is used as well to provide a higher fidelity model compared to the AD model. The effect of model fidelity on optimal design decisions and resulting performance can be analyzed by studying the differences between both these implementation results.

F. ATC Formulation

A bi-level ATC formulation is used for the design optimization of an eVTOL aircraft. The top-level optimization function includes the system level problem formulation and the bottom level performs the optimization of all the individual subsystems. The ATC formulation optimizes for ten design variables, which are defined in Table 1.

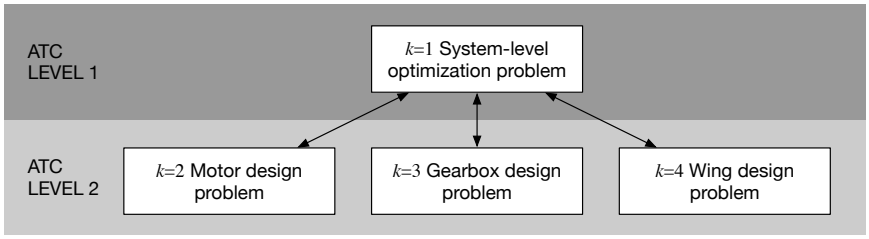

Fig. 3 ATC formulation for eVTOL design

Table 2 List of all shared, local and coupled variables used in eVTOL design formulation using ATC

$x_\#$	Symbol	Classification	$x_\#$	Symbol	Classification
1	r_{prop}	shared variable	6	E_{reserve}	local variable (system)
2	V	shared variable	7	b_{span}	coupled variable (wing)
3	m_{batt}	local variable (system)	8	ω_{hover}	shared variable
4	m_{motor}	coupled variable (motor)	9	η_{motor}	shared variable
5	MTOW	coupled variable (system)	10	m_{gb}	coupled variable (gearbox)

Each component level optimization problem maintains a local copy of all the shared and coupling variables which are interfaced with the system level optimizer, and that are driven toward agreement via penalty functions. All the component level formulations include just the penalty function as the objective function and analysis (or sizing) functions as constraints. A schematic of the ATC formulation structure used here in provided in Fig. 3. The system-level problem is numbered with $k = 1$, whereas the subsystem-level problems are numbered with $k \in [2, 3, 4]$. This numbering is consistent with the formulation introduced in Eq. (1).

The same objectives and constraints are adapted for the multidisciplinary feasible (MDF) formulation, a monolithic MDO problem formulation, against which the optimal solution of ATC is compared. In the MDF formulation, the penalty functions pertaining to consistency constraints are not necessary as only one copy of the design variables exists, and all the other constraints are included in a single optimization formulation with the system level objective from ATC as the sole objective function.

IV. Results

A. Optimal design solution

Distributed optimization using ATC and monolithic optimization using MDF are performed with both higher- (BEM) and lower- (AD) fidelity models for three different ranges. The results are compared against each other in Fig. 4. ATC produces somewhat suboptimal solutions compared to the fully-converged results from MDF. The converged design solutions of the ATC and MDF formulations are very close, meaning that they converged to approximately the same solutions, but with differing solution accuracy levels. However, since the problem is tightly constrained and highly sensitive to each of the design variables, the values of overall mass has significant differences. In all cases, MDF gives superior solutions, while the ATC can provide comparable solutions for certain cases, including the optimal result for 50 km range with the BEM model.

Since distributed MDO approaches involve decomposition of one problem into multiple optimization problems, the solution is to be iteratively converged between formulations, and the convergence rate and solution procedure stability are both highly affected by the parameter values used for augmented Lagrangian penalty function, i.e., β and γ. Analogous to learning rates, a large β value can quickly make the algorithm skip the optimal solution and oscillate between suboptimal points. A strategy was used for this study where the value of beta is slowly reduced as the residual of ATC penalties begin decreasing with each iteration. This helped to ease numerical difficulties in practice.

Computational expense is a predominant disadvantage of the distributed MDO approach here. Table 3 shows

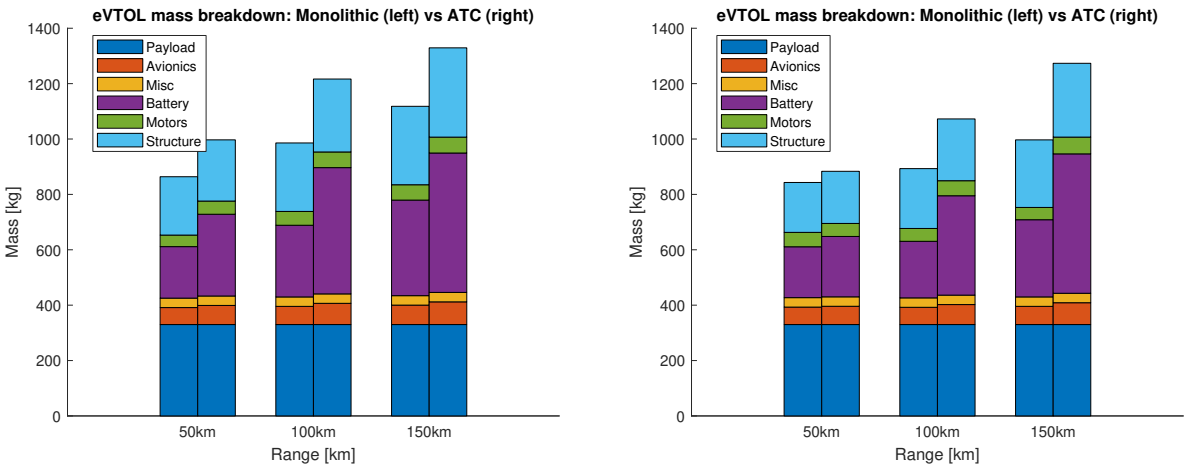

(a) Actuator disk (lower-fidelity) model **(b) Blade element momentum (higher-fidelity) model**

Fig. 4 MDF vs ATC optimal solution comparison

Table 3 Computational expense comparison

Case	Function evaluations	Computational time
ATC with AD	68968	157 s
MDF with AD	66	17 s
ATC with BEM	97504	210 s
MDF with BEM	62	16 s

the computational time for the aforementioned design optimization cases. A single solution time for the monolithic formulation is typically higher than a single (parallel) set of solution time for ATC subproblems. Even with extensive tuning for fast convergence, the ATC algorithm in this study required more time to converge to a solution than MDF for the same tolerance limits.

B. Design coupling analysis

A design coupling analysis for all the design variables is performed to better understand how we should make design decisions when one design decision changes. The design coupling is defined in the form of Jacobian matrix, given as:

$$\frac{\partial \hat{\mathbf{x}}^*}{\partial \hat{\mathbf{x}}} = \begin{bmatrix} \partial \hat{x}_1^*/\partial \hat{x}_1 & \cdots & \partial \hat{x}_1^*/\partial \hat{x}_{N_x} \\ \vdots & \ddots & \vdots \\ \partial \hat{x}_{N_x}^*/\partial \hat{x}_1 & \cdots & \partial \hat{x}_{N_x}^*/\partial \hat{x}_{N_x} \end{bmatrix}, \tag{12}$$

where $\hat{\mathbf{x}}$ denotes design variable vector normalized with the range between upper and lower bounds, given as:

$$\hat{\mathbf{x}} \equiv \mathbf{x} \oslash (\mathbf{x}_{\text{ub}} - \mathbf{x}_{\text{lb}}), \tag{13}$$

where the $\oslash$ operator denotes Hadamard division (element-wise division of vectors), and N_x denotes the number of design variables. The diagonal components of the design coupling Jacobian matrix will always be one. When taking the logarithm of these diagonal elements, they will be equal to zero, since the logarithm of one is zero. Computing a design coupling Jacobian matrix involves perturbing each design variable by a fixed quantity (one percent of the range between upper and lower bounds in this problem) and the model is optimized again for remaining design variables, while the perturbed design variable is kept fixed. The value of the design coupling Jacobian, in general, changes with design $\mathbf{x}$, so it is a challenging characteristic to quantify and interpret.

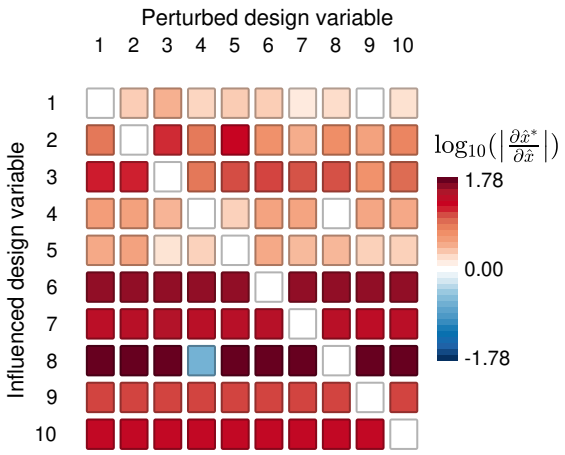

Fig. 5 Colormap representing Jacobian matrix of design coupling for eVTOL optimization problem

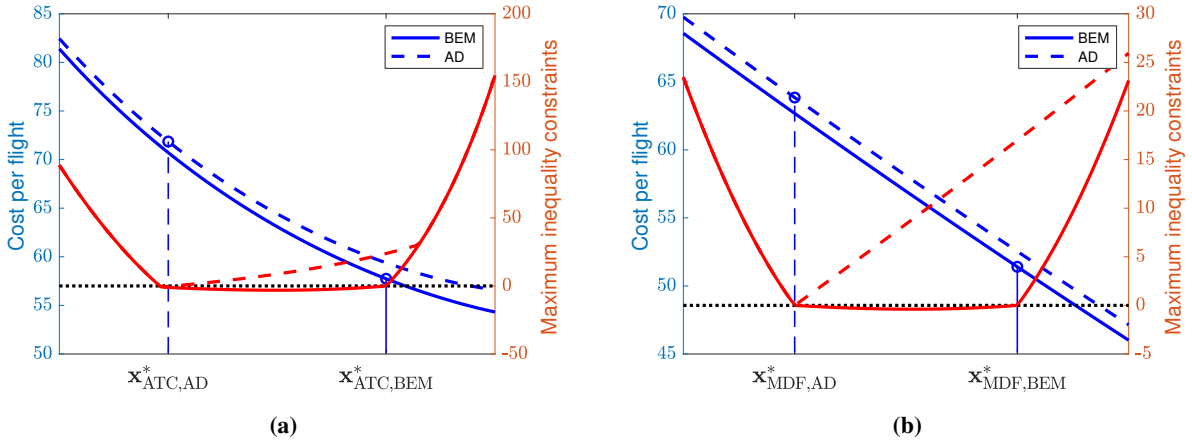

Fig. 6 Comparison of solutions for different model fidelities (AD and BEM)

Figure 5 illustrates the design coupling Jacobian for the 10 variables listed in Table 1 based on the MDF solution with AD model at 150 km range. The Jacobian matrix colormap represents the impact of a perturbed design variable (column numbers) on an influenced variable (row numbers). Warmer colors signify stronger-than-linear coupling, while cooler colors denote weaker-than-linear coupling. White corresponds to linear coupling, and as anticipated, all diagonal elements appear white. The majority of variables exhibit strong coupling. Generally, propeller radius ($x_1 = r_{\text{prop}}$), motor mass ($x_4 = m_{\text{motor}}$), and maximum takeoff weight ($x_5 = \text{MTOW}$) show less sensitivity to other design decisions, while hover rpm ($x_8 = \omega_{\text{hover}}$), reserve mission energy ($x_6 = E_{\text{reserve}}$), wingspan ($x_7 = b_{\text{span}}$), gearbox mass ($x_{10} = m_{\text{gb}}$), and motor efficiency ($x_9 = \eta_{\text{motor}}$) demonstrate higher susceptibility. Although most design choices significantly impact optimal hover rpm, motor mass barely affects it, as indicated by the blue color.

It is also noteworthy that the design coupling Jacobian is diagonally asymmetric, implying that a strong impact from one design variable on another does not guarantee a similarly strong influence in the opposite direction. For example, if x_5 is perturbed, a change in x_3^* is larger than x_4. However, a change in x_5^* is relatively small when x_3 is perturbed, compared to the case when x_4 is perturbed.

C. Model fidelity to design utility analysis

Model fidelity refers to how the model accurately reflects the physical reality. However, higher model fidelity does not necessarily provide superior performance in the perspective of design utility. In this problem, we have two different model fidelity levels (AD and BEM), and two different design methodologies (ATC and MDF); we can analyze and

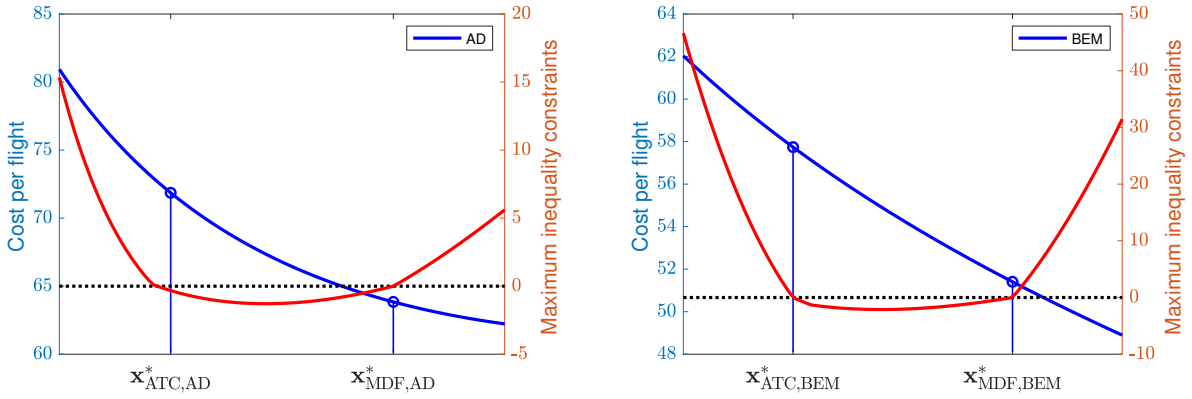

Fig. 7 Comparison of solutions for different design fidelities (ATC and MDF)

compare the design solutions with all combinations.

Figure 6 represents the system model responses cost function (blue lines) and maximum inequality constraints (red lines) by varying design variable vector linearly between two optimal design points with AD and BEM models obtained by (a) ATC and (b) MDF, respectively. The linear variation between n-dimensional design variable vectors $\mathbf{x}^*_A$ and $\mathbf{x}^*_B$ (with 50% of additional ranges outside of the two) are defined is defined as:

$$\mathbf{x}(\lambda) = (1-\lambda)\,\mathbf{x}^*_A + \lambda \mathbf{x}^*_B, \tag{14}$$

for $\lambda \in (-0.5,\ 1.5)$, and this linear variation is a similar concept to line search in optimization procedures.

In Fig. 6(a), the ATC-provided optimal design points are illustrated, along with the trends of the objective function and the maximum values of inequality constraints. These are displayed in the linearly varying subspace between the optimal points obtained using the AD and BEM models. Although the objective and constraint function trends are close to each other, a small disparity in the inequality constraint functions results in a significant difference in the optimal objective function values. Regarding the MDF solutions presented in Fig. 6(b), the difference in feasibility is even more pronounced. Consequently, for design problems with tight constraints, a minor difference in model fidelity can lead to a substantial discrepancy in the optimal solutions.

In Fig. 7, the objective and inequality constraint functions along the linearly varying space between ATC and MDF design solutions is shown. Figure 7(a) shows the solutions using the AD model, while Fig. 7(b) shows the solutions using the BEM model. This figure directly compares the solutions obtained by two different design methodologies: ATC and MDF. In all cases, MDF method provided highly accurate design solutions converged right at the constraint boundary, while the ATC method failed to converge to a solution at the constraint boundary, although the solutions found were all in the feasible design domain. As we consider a design practice executed in structured organizations, the iterative design communications are mostly focused on finding collaborative solutions within feasible design space, while improving performance metric is another important goal. The ATC method is not failing in this goal, but with a higher computational cost than one with monolithic formulations.

D. General purpose ATC solver

Another output of this effort is an open-source general-purpose ATC software package [25]. The hierarchical ATC formulation along with the ALC penalty functions are packaged into a MATLAB application that can be used to solve general ATC optimization problems. The application is demonstrated in the referenced `github` repository using a few algebraic optimization problems such as the Sellar problem [26], which is decomposed into a bilevel ATC formulation.

V. Conclusion

The results highlighted in this article demonstrate the capabilities and limitations of ATC in solving highly coupled engineering design problems, such as the eVTOL aircraft design optimization. Although ATC may incur higher computational costs, the enhanced modularity of this formulation allows for more structured interactions among various

subsystems as compared to monolithic MDO methods.

When implemented at an organizational level, the overall cost of human effort (including formulation construction, formulation analysis, solution analysis, and refinement) could be reduced through the application of such a structure, primarily by minimizing the need to achieve consensus across the full design organization for all problem formulation decisions. Individual engineering teams can focus on solving and refining the assigned subproblems, and costly system-level model refinements are only necessary when interface adjustments are required. Another potential value of using ATC (and decomposition-based methods) is that customized optimization algorithms, such as optimal control, can be employed to efficiently solve specific subproblems, rather than using a general optimization solver for a single monolithic problem.

The eVTOL design problem developed here is a simple and effective benchmark problem for distributed and monolithic MDO formulations. All ten design variables are highly coupled to each other, so design solutions are critically affected by any perturbed design decision. Without an MDO study, design activities of the eVTOL problem cannot achieve high efficiency in the cost of a flight or the overall weight of the flight. The problem presented here is an effective demonstration of the benefit of considering all design disciplinary domains at the same time.

With the comparison of solutions between different fidelity levels and design methodologies, it is apparent that there is a need for a better distributed optimization formulations to support the use of MDO in structured organizations to inform collaborative design practices. Future research topics may include implementing characteristics that make monolithic formulations computationally efficient in the implementation of distributed formulations and their information exchange structures. The ATC application framework developed in this study serves as a good starting point for research extension to more useful distributed MDO formulations, as well as the practical design tool for any type of full-scale multidisciplinary design problems. We expect that more implementations of distributed MDO methods will follow and the work demonstrated in this study aids in this journey.

VI. Acknowledgments

This material is based upon work supported by the National Science Foundation Engineering Research Center for Power Optimization of Electro-Thermal Systems (POETS), United States with cooperative agreement EEC-1449548. This research was made possible by periodic review and suggestions by NASA members Timothy Krantz, Christopher Snyder, Christopher Silva, and Mark Valco. Opinions expressed in this publication are only those of the authors.

References

[1] Schmit Jr., L. A., "Structural design by systematic synthesis," *Proceedings of the 2nd Conference on Electronic Computation*, American Society of Civil Engineers, Pittsburgh, PA, 1960, pp. 105–132.

[2] Livne, E., Schmit, L. A., and Friedmann, P. P., "Towards integrated multidisciplinary synthesis of actively controlled fiber composite wings," *Journal of Aircraft*, Vol. 27, No. 12, 1990, pp. 979–992. https://doi.org/10.2514/3.45972.

[3] Cai, G., Fang, J., Zheng, Y., Tong, X., Chen, J., and Wang, J., "Optimization of system parameters for liquid rocket engines with gas-generator cycles," *Journal of Propulsion and Power*, Vol. 26, No. 1, 2010, pp. 113–119. https://doi.org/10.2514/1.40649.

[4] Agte, J. S., Sobieszczanski-Sobieski, J., and Sandusky Jr., R. R., "Supersonic business jet design through bi-level integrated system synthesis," *SAE Transactions, Section 1: Journal of Aerospace*, Vol. 108, 1999, pp. 1356–1364.

[5] Martins, J. R. R. A., and Lambe, A. B., "Multidisciplinary design optimization: a survey of architectures," *AIAA Journal*, Vol. 51, No. 9, 2013, pp. 2049–2075. https://doi.org/10.2514/1.J051895.

[6] Cramer, E. J., Dennis Jr., J. E., Frank, P. D., Lewis, R. M., and Shubin, G. R., "Problem Formulation for Multidisciplinary Optimization," *SIAM Journal on Optimization*, Vol. 4, No. 4, 1994, pp. 754–776. https://doi.org/10.1137/0804044.

[7] Allison, J. T., "Engineering Design Optimization Course Notes (SE 413)," , January 2023. University of Illinois at Urbana-Champaign.

[8] Guo, T., Herber, D., and Allison, J. T., "Circuit Synthesis Using Generative Adversarial Networks (GANS)," *AIAA Scitech 2019 Forum*, 2019, p. 2350.

[9] Michelena, N., Kim, H. M., and Papalambros, P., "A System Partitioning and Optimization Approach to Target Cascading," *Proceedings of the 12th International Conference on Engineering Design*, Vol. 2, Munich, 1999, pp. 1109–1112.

[10] Michelena, N., Papalambros, P., Park, H. A., and Kulkarni, D., "Hierarchical Overlapping Coordination for Large-scale Optimization by Decomposition," *AIAA journal*, Vol. 37, No. 7, 1999, pp. 890–896.

[11] Kim, H. M., Michelena, N. F., Papalambros, P. Y., and Jiang, T., "Target cascading in optimal system design," *Journal of Mechanical Design*, Vol. 125, No. 3, 2003, pp. 474–480. https://doi.org/10.1115/1.1582501.

[12] Sosa, M. E., Eppinger, S. D., and Rowles, C. M., "The Misalignment of Product Architecture and Organizational Structure in Complex Product Development," *Management science*, Vol. 50, No. 12, 2004, pp. 1674–1689.

[13] Tosserams, S., Etman, L. F. P., Papalambros, P. Y., and Rooda, J. E., "An augmented Lagrangian relaxation for analytical target cascading using the alternating direction method of multipliers," *Structural and Multidisciplinary Optimization*, Vol. 31, No. 3, 2006, pp. 176–189. https://doi.org/10.1007/s00158-005-0579-0.

[14] Silva, C., Johnson, W., Patterson, M. D., and Antcliff, K. R., "VTOL urban air mobility concept vehicles for technology development," *Aviation Technology, Integration, and Operations Conference*, American Institute of Aeronautics and Astronautics, Atlanta, GA, 2018, pp. 1–12. https://doi.org/10.2514/6.2018-3847.

[15] Tosserams, S., Etman, L. F. P., and Rooda, J. E., "Augmented Lagrangian coordination for distributed optimal design in MDO," *International Journal for Numerical Methods in Engineering*, Vol. 73, No. 13, 2008, pp. 1885–1910. https://doi.org/10.1002/nme.2158.

[16] Allison, J. T., Kokkolaras, M., Zawislak, M., and Papalambros, P. Y., "On the Use of Analytical Target Cascading and Collaborative Optimization for Complex System Design," *6th World Congress on Structural and Multidisciplinary Optimization Rio de Janeiro*, Vol. 30, 2005.

[17] Allison, J., Roth, B., Kokkolaras, M., Kroo, I., and Papalambros, P., "Aircraft Family Design Using Decomposition-based Methods," *11th AIAA/ISSMO Multidisciplinary Analysis and Optimization Conference*, 2006, p. 6950.

[18] Lambe, A. B., and Martins, J. R. R. A., "Extensions to the Design Structure Matrix for the Description of Multidisciplinary Design, Analysis, and Optimization Processes," *Structural and Multidisciplinary Optimization*, Vol. 46, No. 2, 2012, pp. 273–284. https://doi.org/10.1007/s00158-012-0763-y.

[19] Warwick, G., "Inside Airbus A3's Vahana electric VTOL," url: https://aviationweek.com/aerospace/aircraft-propulsion/inside-airbus-a3s-vahana-electric-vtol, code: https://github.com/VahanaOpenSource/vahanaTradeStudy, 2017. Accessed: 2023-04-01.

[20] Sarojini, D., Ruh, M. L., Joshy, A. J., Yan, J., Ivanov, A. K., Scotzniovsky, L., Fletcher, A. H., Orndorff, N. C., Sperry, M., Gandarillas, V. E., et al., "Large-Scale Multidisciplinary Design Optimization of an eVTOL Aircraft using Comprehensive Analysis," *AIAA SCITECH 2023 Forum*, 2023, p. 0146.

[21] Hendricks, E. S., Falck, R. D., Gray, J. S., Aretskin-Hariton, E., Ingraham, D., Chapman, J. W., Schnulo, S. L., Chin, J., Jasa, J. P., and Bergeson, J. D., "Multidisciplinary optimization of a turboelectric tiltwing urban air mobility aircraft," *AIAA Aviation Forum*, American Institute of Aeronautics and Astronautics, Dallas, TX, 2019, pp. 1–20. https://doi.org/10.2514/6.2019-3551.

[22] Brown, G. V., Kascak, A. F., Ebihara, B., Johnson, D., Choi, B., Siebert, M., and Buccieri, C., "NASA Glenn Research Center program in high power density motors for aeropropulsion," Technical Report NASA/TM-2005-213800, National Aeronautics and Space Administration, Cleveland, OH, Dec. 2005.

[23] Leishman, J. G., *Principles of Helicopter Aerodynamics*, 2nd ed., Cambridge University Press, Cambridge, 2016.

[24] Anemaat, W. A., Schuurman, M., Liu, W., and Karwas, A. A., "Aerodynamic design, analysis and testing of propellers for small unmanned aerial vehicles," *55th AIAA Aerospace Sciences Meeting*, American Institute of Aeronautics and Astronautics, Grapevine, TX, 2017, pp. 1–12. https://doi.org/10.2514/6.2017-0721.

[25] Chinthoju, P., "ATC application," url: https://github.com/chinthojuprajwal/ATC_application, 2022. Accessed: 2023-04-01.

[26] Sellar, R. S., Batill, S. M., and Renaud, J. E., "Response surface based, concurrent subspace optimization for multidisciplinary system design," *Aerospace Sciences Meeting and Exhibit*, American Institute of Aeronautics and Astronautics, Reno, NV, 1996, pp. 1–14. https://doi.org/10.2514/6.1996-714.